

See discussions, stats, and author profiles for this publication at: <https://www.researchgate.net/publication/26295424>

Rate coefficients for the reaction of OH with $\text{CF}_3\text{CH}_2\text{CH}_3$ (HFC-263fb) between 200 and 400 K: Ab Initio, DFT, and transition state theory calculations

ARTICLE in JOURNAL OF COMPUTATIONAL CHEMISTRY · JANUARY 2009

Impact Factor: 3.59 · DOI: 10.1002/jcc.21336 · Source: PubMed

CITATIONS

9

READS

6

2 AUTHORS:



Akbar Ali Moahamad

University of Michigan

12 PUBLICATIONS 51 CITATIONS

SEE PROFILE



B. Rajakumar

Indian Institute of Technology Madras

37 PUBLICATIONS 243 CITATIONS

SEE PROFILE

Rate Coefficients for the Reaction of OH with CF₃CH₂CH₃ (HFC-263fb) Between 200 and 400 K: *Ab Initio*, DFT, and Transition State Theory Calculations

MOHAMAD AKBAR ALI, B. RAJAKUMAR

Department of Chemistry, Indian Institute of Technology Madras, Chennai 600036, India

Received 13 February 2009; Revised 14 April 2009; Accepted 21 April 2009

DOI 10.1002/jcc.21336

Published online 15 June 2009 in Wiley InterScience (www.interscience.wiley.com).

Abstract: Rate coefficients for the reaction of the hydroxyl radical with CF₃CH₂CH₃ (HFC-263fb) were computed using *ab initio* methods, viz. MP2, G3MP2, and G3B3 theories between 200 and 400 K. Structures of the reactants in the ground state (GS) and transition state (TS) were optimized at MP2(FULL)/6-31G*, MP2(FULL)/6-311++G**, and B3LYP/6-31G* level of theories. Seven TSs were identified for the title reaction in the above theories. However, five out of seven TSs were found to be symmetrically distinct. The kinetic parameters due to these five different TSs are presented in this manuscript. Intrinsic reaction coordinate (IRC) calculations were performed to confirm the existence of transition states. The contributions of all the individual hydrogens in the substrate for the reaction are estimated and compared with the results obtained using Structure Additivity Relationships. The rate coefficients for the title reaction were computed to be $k = (7.96 \pm 0.93) \times 10^{-13} \exp [-(2245 \pm 30)/T] \text{ cm}^3 \text{ molecule}^{-1} \text{ s}^{-1}$ at MP2, $k = (9.50 \pm 0.93) \times 10^{-13} \exp [-(1162 \pm 30)/T] \text{ cm}^3 \text{ molecule}^{-1} \text{ s}^{-1}$ at G3MP2, and $k = (7.01 \pm 0.88) \times 10^{-13} \exp [-(753 \pm 35)/T] \text{ cm}^3 \text{ molecule}^{-1} \text{ s}^{-1}$ at G3B3 theories. The theoretically computed rate coefficients are found to be in excellent agreement with the experimentally determined ones. The OH-driven atmospheric lifetimes of this compound are computed to be 132, 2.2, and 0.7 years at, MP2, G3MP2, and G3B3 level of theories, respectively.

© 2009 Wiley Periodicals, Inc. J Comput Chem 31: 500–509, 2010

Key words: hydrochlorofluorocarbons; *ab initio*; transition state theory; rate coefficients; atmospheric lifetimes

Introduction

The chlorofluorocarbons (CFCs) are proved to be responsible for the stratospheric ozone depletion¹ and greenhouse effects. Because of the extensive usage of the CFCs, researchers were prompted to find the environmentally friendly alternatives to CFCs. Although, hydrochlorofluorocarbons (HCFCs) were immediate replacements to CFCs, the presence of chlorine was not taken well. The next alternatives suggested were hydrofluorocarbons (HFCs). As HFCs do not contain any chlorine or bromine, they do not pose any threat to the stratospheric ozone.² HFCs can be lost in the atmosphere much faster than CFCs via their reaction with hydroxyl radicals (OH) because of the presence of at least one C–H bond. However, to estimate their atmospheric lifetimes, reliable rate coefficients over relevant temperature range are essential.

Although, several research groups have investigated the lifetimes of various compounds by using many advanced techniques, viz. Discharge Flow (DF), Laser Induced Fluorescence (LIF), Pulsed Laser Photolysis (PLP), and Relative methods, theoretical methods always give very valuable inputs. Based on the availability of the experimental rate coefficients, Atkinson and coworker,^{3,4} DeMore,⁵ and Tokuhashi et al.⁶ groups have

independently worked out the Structure Activity Relationships (SARs) to derive the rate coefficients of the reactions of various compounds with OH radicals. But again, these methods are inadequate because of the limited number of experimentally measured rate coefficients. In the event of nonavailability of experimentally measured rate coefficients, the theoretical methods are the only possible resource in determining them. Transition state theory is quite successful in computation of the rate coefficients for these reactions, and is supplemented by *ab initio* methods and density functional theories, which can provide accurate estimates for necessary structural and energetic parameters. Several investigations on the reactions of OH radicals with molecules, such as CFCs, HFCs, chloromethane,⁷ dichloroethane,⁸ fluoromethanes,^{9–16} fluoroethanes,^{17,18} and fluoropropanes¹⁹ have already been reported.

CF₃CH₂CH₃ (HFC-263fb) is one among the many HFCs suggested as potential substitutes to CFCs. To the best of our knowledge, the experimentally measured rate coefficients for its

Additional Supporting Information may be found in the online version of this article.

Correspondence to: B. Rajakumar; e-mail: rajakumar@iitm.ac.in

reaction with OH radical are reported only by two groups.^{20,21} Nelson et al.²⁰ have investigated this reaction using DF technique with Laser Induced Fluorescence (DF-LIF) detection of hydroxyl (OH) radicals at room temperature. The rate coefficient reported by them is $k(298) = (4.20 \pm 0.43) \times 10^{-14}$ cm³ molecule⁻¹ s⁻¹. In another investigation, Ravishankara and co-workers²¹ reported the rate coefficient for this reaction to be $k(T) = (4.36 \pm 0.63) \times 10^{-12} [\exp(-1293 \pm 42)/T]$ cm³ molecule⁻¹ s⁻¹ between 238 and 373 K, and at 298 K the rate coefficient reported was $k(298) = (5.55 \pm 0.48) \times 10^{-14}$ cm³ molecule⁻¹ s⁻¹. In these investigations, they have used Pulsed Laser Photolysis technique with Laser Induced Fluorescence (PLP-LIF) detection of OH. A theoretical investigation by Percival et al.²² has reported the temperature dependence of this reaction to be $3.16 \times 10^{-12} [\exp(-1385)/T]$ cm³ molecule⁻¹ s⁻¹. They have obtained the Arrhenius parameters by correlating the calculated ionization potentials with the recommended kinetic parameters by Atkinson et al.²³ and De More et al.²⁴ Recently, Gonzalez-Lafont et al.²⁵ have used mPW1B95-41.0 hybrid density functional theory^{26–28} with 6-31+G** basis set and canonical variational transition state theory to calculate the rate coefficient for the title reaction. Urata et al.²⁹ have developed somewhat general but, empirical model to estimate the rate coefficients for the reactions of OH radicals with many HFCs and hydrofluoroethers.

In this article, we present the rate coefficients of the reaction of CF₃CH₂CH₃ (HFC-263fb) with OH radical (for which the possible channels are given below) in the temperature range of 200–400 K by using transition state theory and *ab initio* methods MP2 (FULL), G3MP2, and G3B3.



We present geometries, energetics, vibrational frequencies of each stationary point, i.e., reactants, transition states (TSs), and products. We report the rate coefficients due to all possible TSs and also report the overall rate coefficient for the reaction.

Computational Methods

Structure and Energetics

The structures of the reactants 1,1,1-trifluoropropane, (CF₃CH₂CH₃), and OH radical in their ground state (GS) were optimized at the second order Møller-Plesset³⁰ MP2(FULL) including all electrons in correlation, B3LYP functional^{27,31–33} with Pople basis sets 6-311++G** and 6-31G*. Potential energy surface for HFC-263fb molecule was carried out using MP2(FULL)/6-311++G** level of theory and it was found that only one minimum in the staggered form exists. The structures of seven TSs denoted as TS1, TS2, TS3, TS3a, TS4, TS4a, and TS5 (see Fig. 1) were optimized at same level of theories and basis sets³⁴ which are internally available with the Gaussian program suite.³⁵ TS1, TS2, TS3, and TS3a correspond to the abstraction of hydrogen from methyl group (–CH₃), and TS4,

TS4a, and TS5 correspond to the abstraction from methylene hydrogens (–CH₂–). Frequency calculations were carried out for reactants in the GS, TS, and product geometries at the same level of theories and basis sets. All the TSs were identified with one imaginary frequency corresponding to the reaction coordinate. The structures and normal modes were viewed in Gaussview³⁶ and the normal mode corresponding to the reaction coordinate was observed to be consistent with the reaction of interest. Structural parameters obtained from MP2(FULL)³⁰ and Gaussian-3³⁷ methods, namely, G3MP2³⁸ and G3B3,³⁹ were used for all energetic and kinetic calculations.

Rate Coefficients

Rate coefficients for hydrogen abstraction from HFC(–263fb) were calculated using the standard transition state theory.⁴⁰

$$k(T) = l \frac{k_B T}{h} \left(\frac{Q_{\#}}{Q_R} \right) \exp \left(-\frac{\Delta E_0}{RT} \right) \quad (1)$$

where “#” represents the transition state and k_B is the Boltzmann constant. $Q_{\#}$ and Q_R are partition functions for the TS and the reactants in the GS. The electronic partition function of OH radical was evaluated by taking the splitting of 139.7 cm⁻¹ in the ²Π GS, into account.⁴¹

$$Q^E(\text{OH}) = 2 + 2 \exp[-140(\text{cm}^{-1})hc/k_B T] \quad (2)$$

where h is the Planck's constant and c is the velocity of light (3×10^{10} cm s⁻¹). l is the statistical factor (reaction path degeneracy). There have been lot of discussions on reaction path degeneracy and we follow the recommendation by Pollak and Pechukas⁴² as summarized by Gilbert and Smith,⁴³ i.e.,

$$l = \frac{m^{\#} \sigma}{m \sigma^{\#}} \quad (3)$$

where σ is the symmetry number, m is the number of optical isomers.

Quantum mechanical tunneling effects along the reaction coordinate were included by a temperature dependent transmission coefficient $\Gamma(T)$. The final rate coefficients were calculated by

$$k^{\Gamma}(T) = \Gamma(T)k(T) \quad (4)$$

The values of $\Gamma(T)$ were calculated by using Wigner's⁴⁴ method.

$$\Gamma(T) = 1 + \frac{1}{24} \left(\frac{h\nu^*}{k_B T} \right)^2 \quad (5)$$

where ν^* is the imaginary frequency associated with the transition state. This method was very widely used for these abstraction reactions by various research groups.^{7,14,16,45}

The rate coefficients were calculated at every 25 K within the complete temperature range, for all the reported theories.

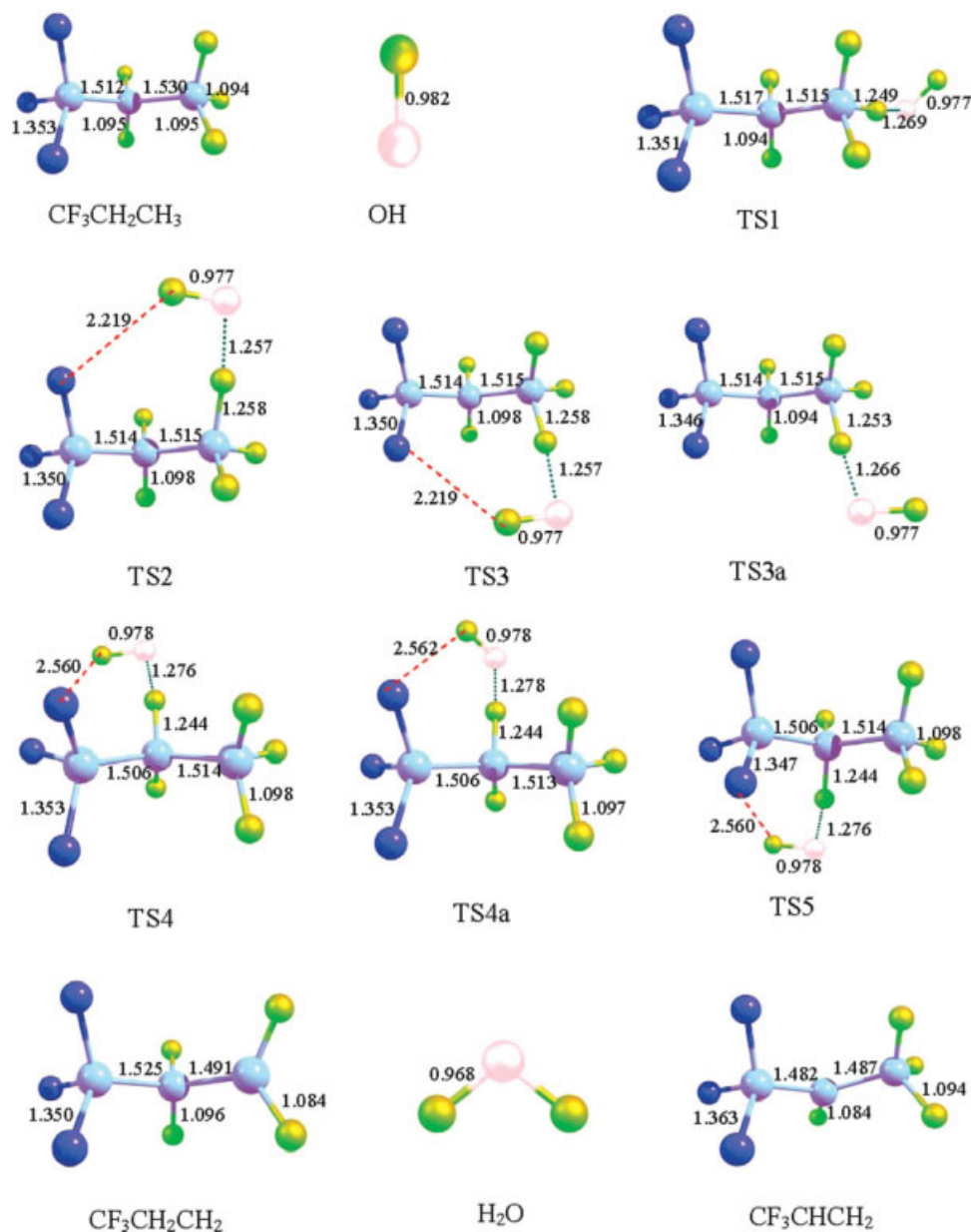


Figure 1. Geometries of the reactants, all transition states, and all products optimized at B3LYP/6-31G* level of the theory. TS2 and TS3 are symmetrically equivalent as are TS4 and TS5. Dark blue represents Fluorine, sky blue represents Carbon, green represents Hydrogen, and pale pink represents oxygen atoms in the structures. The bond lengths (Å) given on the structures are obtained at B3LYP/6-31G* theory.

These calculations were done for only five TSs out of seven, namely, TS1, TS2, TS3a, TS4, and TS4a, *vide infra*.

The thermodynamic formulation of the transition state theory (TST) is then used to estimate E_a and A .

$$k = l \frac{k_B T}{h} \exp \left[\frac{\Delta S^\ddagger}{R} \right] \exp \left[-\frac{E_a}{RT} \right] \quad (6)$$

ΔS^\ddagger is the entropy of activation calculated using the partition functions for the reactant and transition state.

In TST calculations for G3MP2 and MP2(FULL) level of theories, vibrational partition functions of the TS and the reactants were calculated using the vibrational frequencies obtained at MP2 (FULL)/6-311++G**. In the case of G3B3, the vibrational frequencies were obtained at the level of B3LYP/6-31G*. TST calculations were performed using three models, namely, harmonic oscillator (HO) model, free rotor (FR) model, and hindered rotor (HR) model. We have used the method proposed by Truhlar and coworker⁴⁶ to compute the HR partition functions for the lower vibrational modes.

Results and Discussion

Electronic Structure

Structures of CF₃CH₂CH₃, OH radical, and all the seven TSs were optimized at MP2 (FULL)/6-311++G**, MP2 (FULL)/6-31G*, and B3LYP/6-31G* level of theories. HFC-(263fb) has C_s symmetry and contains 2 β and 3 γ hydrogen atoms bonded to carbon atoms. All the structures of the reactants and products in the GS and TSs obtained at B3LYP/6-31G* theory are shown in Figure 1. All the optimized structural parameters of reactants in GS, TSs, and products are given in the Supporting Information Table S-I. Vibrational analysis was done and the vibrational frequencies are given in Supporting Information Table S-II. Imaginary frequencies in the TSs correspond to the abstraction of H by the OH radical. Although there are minor variations in the bond angles and dihedral angles of the reactants among these theories, no significant discrepancies are noted in the C—H, C—F, C—C, and O—H (in OH radical) bond lengths. In the transition state, the important structural parameters have to be observed are one of the C—H bonds of the leaving hydrogen and the newly formed bond between H and O atoms in the OH radical. In Table 1, the differences in bond lengths of the C—H and O—H bonds between the transition state and the reactant are expressed as percentages relative to the reactant. The leaving C—H bond length seems to have varied from 8% to a maximum of 13% in case of all the TSs in all level of theories together. However, in the case of the newly formed bond, i.e., H—O bond, the bond length is varied between 24% and 28%. Also, there is almost no variation in the change in bond length (both C—H and O—H) from TS1 through TS5 at any given individual theory. In the process of optimization of TSs, it is noticed that

hydrogen bond formation between the H atom (of OH radical) and one of the F atoms in the molecule is quite likely. Hence a thorough investigation was carried out to explore all possible TSs. Four TSs were observed (denoted by TS1, TS2, TS3, and TS3a) for the abstraction of hydrogen atoms from —CH₃ group (γ -carbon) and three TSs (denoted by TS4, TS4a, and TS5) for the abstraction from —CH₂— group (β -carbon). To formulate these TSs even more firmly, we have carried out Intrinsic Reaction Coordinate (IRC) analysis in both the directions using TSs at the B3LYP/6-31G(d) theory for hydrogen abstraction process. The IRC calculations were performed in 13 steps for all transition states TS1, TS2, TS3, TS3a, TS4, TS4a, and TS5 (step length = 0.05). At the final step of the calculation, the breaking C—H bond length becomes nearly 1.546 Å whereas the forming O—H bond length becomes 0.999 Å just like in water molecule (0.968 Å). The energies of reactants and products obtained in the IRC calculations are given in Table 2 and they are in excellent agreement with the individually optimized values. Although seven TSs were identified, the transition states TS2 and TS3 as well as TS4 and TS5 were found to have the identical reaction paths. Also, TS2 and TS3, and TS4 and TS5 were observed to have same symmetry. Hence, only five TSs (TS1, TS2, TS3a, TS4, and TS4a) were considered as independent TSs and the rest of the two were not used in the rate coefficient calculations, *vide infra*. Figure 2 depicts the energy profile of these five transition states.

The major structural difference among TSs is due to the presence or absence of hydrogen bonding between the OH hydrogen atom and one of the fluorine atoms in CF₃CH₂CH₃. It has been observed¹⁹ that the hydrogen bonding has significant influence on TSs in hydrogen abstraction reaction from fluorinated alkanes. Here, three TSs have been observed as hydrogen bonded

Table 1. Summary of C—H and O—H Bond Distances (Å) and % Changes Calculated for All the Transition States for H Abstraction From CF₃CH₂CH₃ by OH Radical.

Transition state	Bond	MP2(FULL)/6-311++G**	MP2(FULL)/6-31G*	B3LYP/6-31G*
TS1	C—H (GS) ^a	1.091	1.091	1.094
	O—H (GS) ^b	0.959	0.968	0.968
	C—H (TS)	1.184 (+8%)	1.217 (+10%)	1.249 (+12%)
TS2	O—H (TS)	1.327 (+28%)	1.281 (+24%)	1.269 (+24%)
	C—H (TS)	1.191 (+8 %)	1.223 (+11%)	1.258 (+13%)
TS3	O—H (TS)	1.315 (+27%)	1.270 (+24%)	1.257 (+23%)
	C—H (TS)	1.191 (+8 %)	1.223 (+11 %)	1.258 (+13 %)
TS3a	O—H (TS)	1.315 (+27%)	1.270 (+24%)	1.257 (+23%)
	C—H (TS)	1.189 (+8%)	1.219 (+11%)	1.257 (+13%)
TS4	O—H (TS)	1.322 (+27%)	1.278 (+24%)	1.266 (+24%)
	C—H (TS)	1.192 (+8%)	1.225 (+11%)	1.244 (+12%)
TS4a	O—H (TS)	1.308 (+27%)	1.266 (+24%)	1.276 (+24%)
	C—H (TS)	1.195 (+9%)	1.227 (+11%)	1.244 (+12%)
TS5	O—H (TS)	1.307 (+26%)	1.266 (+24%)	1.278 (+24%)
	C—H (TS)	1.192 (+8%)	1.225 (+11%)	1.244 (+12%)
	O—H (TS)	1.308 (+27%)	1.265 (+24%)	1.276 (+24%)

^aC—H bond length (the leaving hydrogen) in the reactant in its ground state.

^bThe actual O—H bond length in H₂O at the corresponding theories. The numbers in given in the parentheses corresponds to the % change in the bond length in transition state when compared the same bond length in the ground state.

Table 2. Energies (Hartree) of Reactants and Products Obtained in IRC Calculations at B3LYP/6-31G* Level of Theory.

IRC calculations			[B3LYP/6-31G*] ^a					
Reactant		Product	Reactants			Products		
TSs	CF ₃ CH ₂ CH ₃ + OH		OH	CF ₃ CH ₂ CH ₃	Sum	H ₂ O	Radical	Sum
TS1	-492.593	-492.598	-75.723	-416.869	-492.593	-76.409	416.195	-492.604
TS2	-492.593	-492.599	-75.723	-416.869	-492.593	-76.409	-416.195	-492.604
TS3	-492.594	-492.600	-75.723	-416.869	-492.593	-76.409	-416.195	-492.604
TS3 ^a	-492.590	-492.597	-75.723	-416.869	-492.593	-76.409	-416.195	-492.604
TS4	-492.593	-492.600	-75.723	-416.869	-492.593	-76.409	-416.200	-492.608
TS4 ^a	-492.593	-492.601	-75.723	-416.869	-492.593	-76.409	-416.200	-492.608
TS5	-492.593	-492.601	-75.723	-416.869	-492.593	-76.409	-416.200	-492.608

^aThese energies are obtained for individual species at B3LYP/6-31G* level of theory.

TS (TS2, TS4, and TS4a) and two as having no hydrogen bonding TS (TS1, TS3a).

Energetics

The energies in Hartree for the reactants and products in GS and TSs at all level of theories are given in Supporting Information Table S-III. The entropy of activation and barrier heights for the reaction are listed in Table 3. Barrier heights are calculated from the energy (including ZPVE) difference between the TS and GS (CF₃CH₂CH₃, OH) molecules. The activation barriers obtained at MP2(FULL)/6-311++G** level of theory are found to be relatively large when compared with G3MP2 and G3B3 level of theories. The barriers are reduced by 2 kcal mol⁻¹ at G3MP2 and 3 kcal mol⁻¹ at G3B3 theories when compared with the barriers obtained at MP2(FULL)/6-311++G** level of theory. The results obtained using G3B3 are in excellent agreement with the experimental results.²¹ These results are discussed in depth in Kinetic Parameter section. It may be noted here that, the activation barriers for TS2 and TS3, and TS4 and TS5 are just identical.

The activation barriers were reflected very clearly with the kind of TSs (hydrogen bonded and non hydrogen bonded). As mentioned earlier, only five “real” TSs are possible for the title reaction, the discussion is restricted to these five TSs, namely, TS1, TS2, TS3a, TS4, and TS4a. Out of these five transition states, three TSs (TS2, TS4, and TS4a) are influenced by hydrogen bonding between H of OH and one of the near by “F” atoms in the reactant, i.e., CF₃CH₂CH₃ (clear from Fig. 1) and two TSs (TS1 and TS3a) are not influenced by hydrogen bonding. The influence of the hydrogen bonding is clearly seen in the activation barriers. For example, at G3B3 level of theory, the activation energies of TS2, TS4, and TS4a are lower than those of TS1 and TS3a. The barrier height of TS1 (3.32 kcal mol⁻¹) is lower than that of TS3a (4.02 kcal mol⁻¹). It may be due to electrostatic interaction between F and O atom making TS3a higher in energy than TS1. The energy level diagrams for the reaction through R1 and R2 channels via all these five TSs are given in Figure 3. All energies quoted in the Figure 3 are obtained at G3B3 level of the theory. From Table 3, it is clear that the entropy of activation

(ΔS[#]) for the nonhydrogen bonded TSs, namely, TS1 and TS3a are higher than those of hydrogen bonded TSs, namely, TS2, TS4, and TS4a. As a result the pre-exponential factors for the reactions happening through nonhydrogen bonded TSs are larger than the reactions happening through hydrogen bonded TSs. The Arrhenius parameters for all the TSs are tabulated in the Table 4. The standard enthalpy, free energy, and entropy change of the reaction through channel 1 (R1) and through channel 2 (R2) are given in Table 5. The reaction channel R2 is found to be more exothermic when compared with R1.

Kinetic Parameters

Theoretical rate coefficients for the title reaction are calculated using the TST, at all the mentioned theories. The optimized structural parameters and vibrational frequencies used in the TST calculations at MP2 (FULL)/6-311++G** and G3MP2

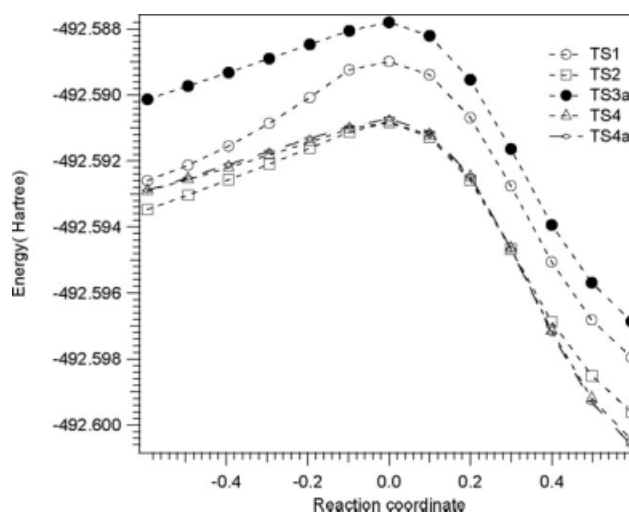


Figure 2. Energy level diagram obtained using IRC calculations at B3LYP/6-31G* level of the theory. The IRC calculations were performed in 13 steps for five transition states, namely, TS1, TS2, TS3a, TS4, and TS4a.

Table 3. Barrier Heights (ΔE_0^\ddagger in kcal mol⁻¹) and Entropy of Activation (ΔS^\ddagger in cal mol⁻¹ K⁻¹) Obtained From Various Levels of Theories.

Reaction channel	TSs	ΔE_0^\ddagger			ΔS^\ddagger (298 K)	
		MP2	G3MP2	G3B3	MP2	G3B3
R1	TS1	6.62	4.65	3.32	-26.51	-26.41
	TS2	6.08	4.12	2.70	-29.68	-29.56
	TS3	6.08	4.12	2.70	-29.68	-29.56
	TS3a	7.48	5.40	4.02	-27.04	-26.89
R2	TS4	5.94	3.85	2.77	-28.54	-28.30
	TS4a	6.14	4.23	3.03	-28.50	-28.60
	TS5	5.94	3.85	2.77	-28.54	-28.30

The TS1 and TS3a values in bold fonts indicate differentiation from the rest of the transition states, as these two transition states are not influenced by hydrogen bonding.

level of the theories were obtained from MP2 (FULL)/6-311++G** and for G3B3 level calculations they were obtained from the optimization at B3LYP/6-31G*. However, the barriers for all the TSs were obtained at the individual level of theories. The calculations were carried out in the temperature range of 200–400 K with 25 K intervals.

As discussed earlier, the reaction goes through two main channels, namely, R1 and R2 (hydrogen abstraction from methyl and methylene groups results in two different product radicals, CF₃CH₂CH₂ and CF₃CHCH₃, respectively). Of the seven TSs obtained, only distinctly different five TSs (TS1, TS2, TS3a, TS4, and TS4a) were used in our TST calculations. The contribution of other two TSs (TS3 and TS5) to the rate coefficient is accounted by multiplying the rate coefficients obtained

by using TS2 and TS4 (These two TSs were in energetic and symmetric equilibrium with TS3 and TS5, respectively) by a factor of 2. The global rate coefficient obtained by summing the rate coefficients computed using this procedure.

We have used three different models to compute the rate coefficients. The torsional motion was treated as either HO or FR or as HR for the calculation of pre-exponential factors. The pre-exponential factors depend largely on the partition functions of the reactants and TSs, and the kind of model that is opted in the calculations. Two lower frequencies of the reactant in the GS and three lower frequencies in all the TSs were treated as HRs. The barriers for these rotors were computed and it was found that only these lower vibrations needed to be treated as HRs. All these lower vibrational frequencies of both reactant and the TSs at all the levels of the theories are listed in the Supporting Information Table S-IV.

Rate coefficients computed using all models at all levels of theories are plotted in Figure 4. The Arrhenius parameters obtained by an unweighted linear least squares fit to all the data are given in the Table 6. The experimentally measured²¹ activation energy for this title reaction is 2590 cal mol⁻¹. The activation energies (E_a 's) predicted by G3B3 level of theory are very close to the experimental values when HO and FR models are used in the computation. However, E_a 's predicted by the other two theories, namely, MP2 (FULL) and G3MP2 are higher when HO and FR models are used. When the HR model is used in all the above theories, the E_a 's were reduced significantly. The pre-exponential factors obtained using HO model are reasonably close to the experimentally measured ones at all the levels of theories. When the torsional motion is treated as a free rotor, the pre-exponential factors are reduced significantly (almost by 50%). The pre-exponential factors obtained using HR

Table 4. Arrhenius Parameters for the Reaction Through all Five Transition States with all the Models Used for the TST Calculations.

Reaction channel	TS	Model	MP2		G3MP2		G3B3	
			$A \times 10^{-13}$ (cm ³ molecule ⁻¹ s ⁻¹)	E_a (kcal mol ⁻¹)	$A \times 10^{-13}$ (cm ³ molecule ⁻¹ s ⁻¹)	E_a (kcal mol ⁻¹)	$A \times 10^{-13}$ (cm ³ molecule ⁻¹ s ⁻¹)	E_a (kcal mol ⁻¹)
R1	TS1	HO	2.25 ± 0.23^a	6.20 ± 0.05	2.87 ± 0.18	4.13 ± 0.03	1.95 ± 0.27	3.77 ± 0.09
		HR	1.79 ± 0.15	4.87 ± 0.03	2.30 ± 0.07	2.81 ± 0.01	1.53 ± 0.16	1.70 ± 0.05
		FR	0.65 ± 0.04	5.84 ± 0.03	0.83 ± 0.02	3.78 ± 0.01	0.51 ± 0.05	2.70 ± 0.05
	TS2	HO	1.24 ± 0.10	5.40 ± 0.04	1.58 ± 0.09	3.36 ± 0.02	1.08 ± 0.14	2.92 ± 0.09
		HR	1.00 ± 0.05	4.64 ± 0.03	1.26 ± 0.03	2.59 ± 0.01	0.83 ± 0.08	1.37 ± 0.05
		FR	0.60 ± 0.02	5.12 ± 0.02	0.75 ± 0.02	3.07 ± 0.01	0.50 ± 0.04	1.90 ± 0.05
	TS3a	HO	4.47 ± 0.41	6.99 ± 0.08	5.69 ± 0.38	4.84 ± 0.03	1.86 ± 0.24	4.40 ± 0.09
		HR	3.60 ± 0.25	6.22 ± 0.03	4.57 ± 0.20	4.07 ± 0.02	1.42 ± 0.14	2.87 ± 0.05
		FR	2.15 ± 0.14	6.70 ± 0.03	2.75 ± 0.08	4.55 ± 0.01	0.85 ± 0.07	3.40 ± 0.05
R2	TS4	HO	1.47 ± 0.14	5.46 ± 0.50	1.83 ± 0.12	3.28 ± 0.03	1.32 ± 0.19	3.19 ± 0.09
		HR	1.45 ± 0.13	4.21 ± 0.05	1.82 ± 0.12	2.03 ± 0.03	1.24 ± 0.19	1.41 ± 0.07
		FR	0.81 ± 0.05	5.16 ± 0.03	1.01 ± 0.03	2.98 ± 0.02	0.66 ± 0.06	2.18 ± 0.05
	TS4a	HO	1.58 ± 0.26	6.05 ± 0.09	1.95 ± 0.26	4.02 ± 0.07	1.11 ± 0.15	3.40 ± 0.08
		HR	1.56 ± 0.24	4.80 ± 0.08	1.95 ± 0.26	2.77 ± 0.07	1.05 ± 0.12	1.62 ± 0.06
		FR	0.88 ± 0.10	5.75 ± 0.06	1.08 ± 0.10	3.72 ± 0.05	0.56 ± 0.05	2.39 ± 0.05

^aThe quoted uncertainties are the 2σ (95% confidence limits) precision from the linear least squares fit of the kinetic parameters obtained for the reaction through each transition state. The TS1 and TS3a values in bold fonts indicate differentiation from the rest of the TSs, as these two TSs are not influenced by hydrogen bonding.

Table 5. Heat of Reaction [ΔH^0 (298 K) in kcal mol⁻¹], Gibbs Free Energy [ΔG^0 (298 K) in kcal mol⁻¹] and Entropy of Reaction [ΔS^0 (298 K) in cal mol⁻¹ K⁻¹].

Theory	ΔH^0 (298 K)	ΔG^0 (298 K)	ΔS^0 (298 K)
Reaction 1			
MP2	-16.81	-18.61	6.06
G3MP2	-15.08	-16.82	5.85
G3B3	-15.50	-17.29	6.01
Reaction 2			
MP2	-17.17	-19.46	7.69
G3MP2	-15.49	-17.63	7.17
G3B3	-15.82	-18.12	7.74

models are falling in the range of pre-exponential factors obtained by HO and FR models.

As stated in the introduction, only two experimental measurements are available for this reaction. One study is done by the corresponding author of this article with Ravishankara's group²¹ and the other one is by Nelson et al.²⁰ It is a known fact that only the global rate coefficient can be measured experimentally. Hence it is worth comparing the measured rate coefficients at room temperature with the theoretically obtained rate coefficients. The experimentally measured room temperature (298 K) rate coefficient (k_{RT}) reported by Ravishankara and coworkers²¹ is $(5.55 \pm 0.48) \times 10^{-14}$ cm³ molecule⁻¹ s⁻¹. Nelson et al.²⁰ reported it to be $(4.20 \pm 0.43) \times 10^{-14}$ cm³ molecule⁻¹ s⁻¹. The global rate coefficients obtained at 300 K in our calculations at all the levels of theories and models are tabulated in Table 7. Rate coefficient obtained using G3B3 level of theory and HR model is $(5.47 \times 10^{-14}$ cm³ molecule⁻¹ s⁻¹) in excellent agreement with the rate coefficient reported by Ravishankara and coworkers,²¹ and it is in reasonable agreement with the one reported by Nelson et al.²⁰ Also, this rate coefficient falls in the vicinity of the rate coefficient reported by Percival et al.²² (3.09×10^{-14} cm³ molecule⁻¹ s⁻¹) at 300 K. Percival et al.²² have calculated Arrhenius parameters based on correlations with calculated ionization potentials of HFCs. Recently Gonzalez-Lafont et al.²⁵ have reported a value of k_{RT} as 4.30×10^{-14} cm³ molecule⁻¹ s⁻¹ by using mPW1B95-41.0 hybrid meta density functional and canonical variational transition state theory in the temperature range of 200 and 373 K. The difference between their approach and ours is that, we have reported

ab initio methods (MP2, G3MP2, and G3B3 in conjugation with B3LYP functional) to obtain the reaction energies.

The rate coefficients obtained at MP2 level of theory in HO and FR models are off by at least three orders of magnitude from the experimental value (see in Table 7). When the torsional motion is treated as the HR, it is improved by an order of magnitude. A similar trend is observed at G3MP2 level of calculations, and in the HR model, the rate coefficient obtained (1.92×10^{-14} cm³ molecule⁻¹ s⁻¹) is closer to the experimentally measured one.^{20,21} The rate coefficients obtained at G3B3 level of theory in HO and FR models are off by 79% and 84%, respectively, from the experimentally measured one. When the torsional motion is treated as the HR, the value obtained is in excellent agreement with the experimentally measured one. Hence, from the above discussion we believe that G3B3 level of theory provides barriers which are very close to the experimentally measured activation energies, by treating the torsional motion as HR, which improves significantly the pre exponential factors. Hence kinetic parameters obtained in combination of G3B3 level of theory and HR model for the abstraction reactions of OH radicals with fluorinated hydrocarbons give reliable kinetic parameters.

We have used Structure Additivity Relationships (SARs) developed by Tokuhashi and coworkers⁶ to estimate the branching ratios of both the reaction channels R1 and R2 and hence the global rate coefficient at 298 K. These methods were developed purely on the available experimental kinetic parameters of varieties of molecules. The rate coefficients obtained for channels R1 and R2 using SAR method are predicted to be 4.16×10^{-14} cm³ molecule⁻¹ s⁻¹ and 2.75×10^{-15} cm³ molecule⁻¹ s⁻¹ respectively (Table 7). The global rate coefficient obtained using this SAR method is 4.4×10^{-14} cm³ molecule⁻¹ s⁻¹. The contribution of CH₃ group to the reaction is calculated to be 94% and that of CH₂ group is 6%. This rate coefficient is in very good agreement with the experimentally measured one by Ravishankara and coworkers,²¹ and Nelson et al.²⁰ We have also computed the rate coefficients for both the channels using the SAR method developed by DeMore's group.⁵ These calculations have shown almost equal contribution from both CH₂ and CH₃ groups. The values obtained by Tokuhashi's SAR method⁶ are not at all in agreement, as far as the CH₂ and CH₃ group contributions are concerned. However, the global rate coefficient estimated using their method is in very good agreement with our results. Gonzalez-Lafont and coworkers²⁵ have reported that, by using the revised

Table 6. Arrhenius Parameters for the Title Reaction CF₃CH₂CH₃ + OH at all the Levels of Theory and all the Models Used in the Calculations.

Model	G3B3		G3MP2		MP2		Experiment ²¹	
	$A \times 10^{-13}$ (cm ³ molecule ⁻¹ s ⁻¹)	E_a/R (K)	$A \times 10^{-13}$ (cm ³ molecule ⁻¹ s ⁻¹)	E_a/R (K)	$A \times 10^{-13}$ (cm ³ molecule ⁻¹ s ⁻¹)	E_a/R (K)	$A \times 10^{-12}$ (cm ³ molecule ⁻¹ s ⁻¹)	E_a/R (K)
HO	7.52 ± 1.22^a	1233 ± 45	11.6 ± 1.18	1759 ± 28	9.33 ± 1.19	2823 ± 35	4.36 ± 0.6	1293 ± 40
HR	7.01 ± 0.88	753 ± 35	9.50 ± 0.93	1162 ± 27	7.96 ± 0.93	2245 ± 33		
FR	3.38 ± 0.39	1076 ± 32	5.61 ± 0.34	1597 ± 17	4.52 ± 0.38	2664 ± 24		

^aThe quoted uncertainties are the 2 σ (95% confidence limits) precision from the linear least squares fit of the kinetic parameters obtained for the reaction through each transition state.

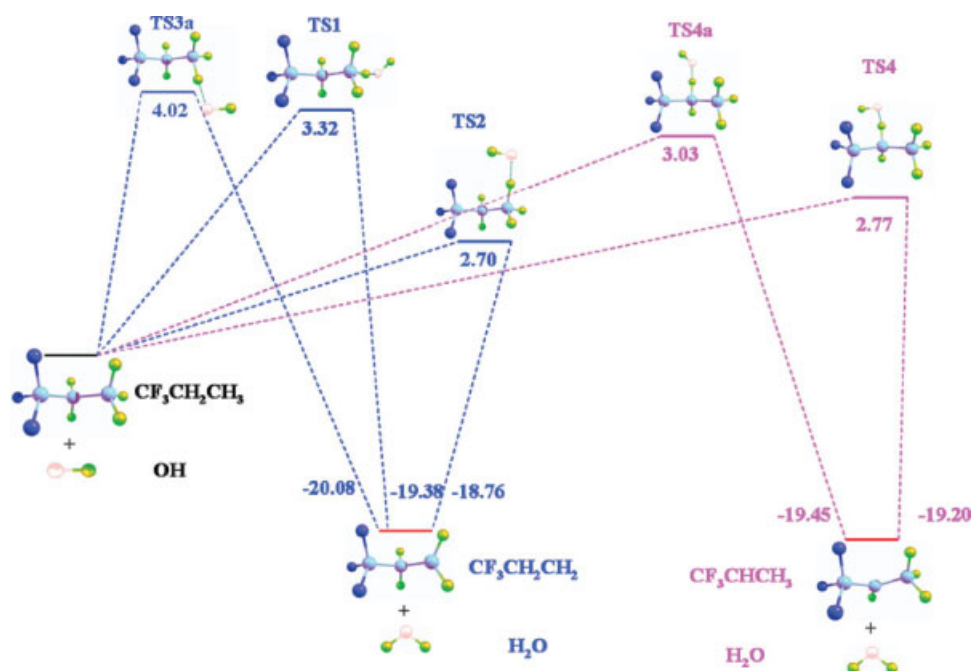


Figure 3. Energy level diagram for the reaction through all the five transition states and both the reaction channels R1 (blue) and R2 (purple), obtained at G3B3 theory.

SAR numbers by DeMore and coworkers the contribution from CH_2 group to be 45% and from CH_3 group to be 55%. In this article, in addition to the contribution of both the reaction channels R1 and R2 to the global rate coefficient, we have also com-

puted the contribution of each hydrogen at all the levels of theories and all the models to global rate coefficient at all the temperatures. The contributions of all the hydrogens at 300 K at all the levels of theories and models are tabulated in Table 7.

Atmospheric Lifetimes

The atmospheric lifetime of any compound that is released into the atmosphere depends on the rates of all processes that remove it viz. reaction with free radicals (exclusively with OH radicals, as they are the most abundant and powerful oxidizing agents in the troposphere), photolysis, and many other processes like dry and wet deposition, rain out, etc. The photolytic loss rate of $\text{CF}_3\text{CH}_2\text{CH}_3$ is negligible, as the UV absorption cross-sections are measured²¹ to be very small, at the wavelengths greater than 300 nm. Therefore, $\text{CF}_3\text{CH}_2\text{CH}_3$ is lost in the atmosphere mainly via its reaction with OH radicals because of the presence of C—H bonds in it. Atmospheric lifetime of any volatile

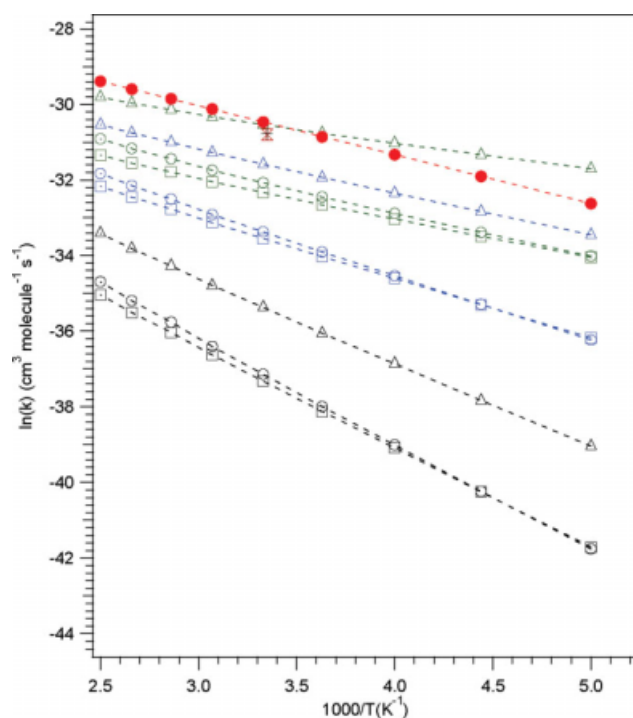


Figure 4. Arrhenius plot for the rate coefficient data obtained for the OH radical reaction with $\text{CF}_3\text{CH}_2\text{CH}_3$ over the temperature range of 200–400 K. The labels with green color correspond to the data obtained at G3B3 theory, blue color correspond to G3MP2 theory and black color correspond to MP2 level of theory. \circ represents the data for HO model, \triangle represents the data for HR model, and \square corresponds to FR model at all levels of theories. The red colored circles are the data obtained using the rate expression derived experimentally by Ravishankara and coworkers.²¹ The symbol “ \times ” in red color represents the rate coefficient reported by Nelson et al.²⁰ The symbol “+” in black color represents the rate coefficient reported by Gonzalez-Lafont et al.²⁵

Table 7. The Rate Coefficients for the Reaction Through all the Transition States at 300 K at all Levels of Theories and all the Three Models.

Method	TS1	TS2	TS3a	SUM R1 ^a	TS4	TS4a	SUM R2 ^b	GLOBAL ^c
	From methyl (−CH ₃) group				From methylene (−CH ₂ −) group			
SAR ^d	4.16 × 10 ^{−14} (93.8%)				2.75 × 10 ^{−15} (6.20%)			4.44 × 10 ^{−14}
HO								
MP2	6.69 × 10 ^{−18}	2.80 × 10 ^{−17}	3.52 × 10 ^{−18}	3.82 × 10 ^{−17}	3.01 × 10 ^{−17}	5.91 × 10 ^{−18}	3.60 × 10 ^{−17}	7.42 × 10 ^{−17}
% ^e	9	38	5	52	40	8	48	100
G3MP2	2.74 × 10 ^{−16}	1.10 × 10 ^{−15}	1.67 × 10 ^{−16}	1.54 × 10 ^{−15}	1.45 × 10 ^{−15}	2.21 × 10 ^{−16}	1.67 × 10 ^{−15}	3.21 × 10 ^{−15}
%	9	34	5	48	45	7	52	100
G3B3	1.10 × 10 ^{−15}	5.28 × 10 ^{−15}	3.72 × 10 ^{−16}	6.75 × 10 ^{−15}	3.87 × 10 ^{−15}	1.16 × 10 ^{−15}	5.03 × 10 ^{−15}	1.18 × 10 ^{−14}
%	9	45	3	57	33	10	43	100
HR								
MP2	4.97 × 10 ^{−17}	8.27 × 10 ^{−17}	1.04 × 10 ^{−17}	1.42 × 10 ^{−16}	2.44 × 10 ^{−16}	4.78 × 10 ^{−17}	2.91 × 10 ^{−16}	4.33 × 10 ^{−16}
%	12	19	2	33	56	11	67	100
G3MP2	2.03 × 10 ^{−15}	3.25 × 10 ^{−15}	4.91 × 10 ^{−16}	5.77 × 10 ^{−15}	1.17 × 10 ^{−14}	1.79 × 10 ^{−15}	1.34 × 10 ^{−14}	1.92 × 10 ^{−14}
%	10	17	3	30	61	9	70	100
G3B3	8.51 × 10 ^{−15}	1.60 × 10 ^{−14}	1.12 × 10 ^{−15}	2.56 × 10 ^{−14}	2.24 × 10 ^{−14}	6.75 × 10 ^{−15}	2.91 × 10 ^{−14}	5.47 × 10 ^{−14}
%	16	29	2.0	47	41	12	53	100
FR								
MP2	3.57 × 10 ^{−18}	2.21 × 10 ^{−17}	2.78 × 10 ^{−18}	2.85 × 10 ^{−17}	2.80 × 10 ^{−17}	5.50 × 10 ^{−18}	3.35 × 10 ^{−17}	6.20 × 10 ^{−17}
%	6	36	4	46	45	9	54	100
G3MP2	1.46 × 10 ^{−16}	8.68 × 10 ^{−16}	1.31 × 10 ^{−16}	1.14 × 10 ^{−15}	1.34 × 10 ^{−15}	2.05 × 10 ^{−16}	1.54 × 10 ^{−15}	2.68 × 10 ^{−15}
%	5	32	5	42	50	8	58	100
G3B3	5.44 × 10 ^{−16}	3.97 × 10 ^{−15}	2.79 × 10 ^{−16}	4.79 × 10 ^{−15}	3.30 × 10 ^{−15}	9.91 × 10 ^{−16}	4.29 × 10 ^{−15}	9.08 × 10 ^{−15}
%	6	44	3	53	36	11	47	100

^aTotal rate coefficient for the reaction through channel one (R1).^bTotal rate coefficient for the reaction through channel two (R2).^cThe global rate coefficient because of both the reaction channels (R1 + R2).^dThe rate coefficients computed using Takahashi's Structure Additivity Relationships (SAR).^eThe percentage contribution of each transition state to the global rate coefficient; Units of k : cm³ molecule^{−1} s^{−1} (given in italic fonts).

organic compound (VOC) degraded largely by the reaction with OH can be best evaluated using global OH concentrations derived from methyl chloroform measurements.^{47,48} We use the OH values and general approach given by Prinn et al.⁴⁸ to derive OH-driven lifetimes of CF₃CH₂CH₃. We have used the rate coefficients computed at different levels of theories with HR model, as this model has given the best results when compared with the other two models (HO and FR). The lifetimes of CF₃CH₂CH₃ estimated by MP2, G3MP2, and G3B3 level of theories are 132, 2.2, and 0.7 years, respectively. The reported OH-driven atmospheric lifetime of CF₃CH₂CH₃ by Ravishankara and coworkers²¹ is 0.8 years. The atmospheric lifetime of CF₃CH₂CH₃ obtained by G3B3 level of theory is in excellent agreement with the experimentally estimated one.

Conclusions

In this article, the rate coefficients for the reaction of CF₃CH₂CH₃ with OH radicals have been reported by using various levels of theories based on *ab initio* and DFT methods. All possible reaction pathways are explored. The results obtained at G3B3 level of theory with the HR approach are in excellent

agreement with the experimentally and theoretically reported ones. We have compared our results with the rate coefficients obtained using various SAR methods. We have also reported the OH driven atmospheric lifetimes of CF₃CH₂CH₃, based on the kinetic parameters obtained in this work and compared with the experimentally estimated ones.

Acknowledgments

All calculations reported in this article were carried out at the Computer Center of IIT Madras. The authors thank the center for valuable support. We thank Dr. Mangala Sunder Krishnan, Department of Chemistry, IIT Madras for useful discussions.

References

1. WMO Scientific Assessment of Ozone Depletion 2002; Global Ozone Research Monitoring Project No. 47, Geneva, 2003.
2. Ravishankara, A. R.; Turnipseed, A. A.; Jensen, N. R.; Barone, S.; Mills, M. C.; Howard, J.; Solomon, S. *Science* 1994, 263, 71.
3. Atkinson, R. *Int. J. Chem Kinet* 1987, 19, 799.
4. Kwok, E. S. C.; Atkinson, R. *Atmos Environ* 1995, 29, 1685.
5. DeMore, W. B. *J Phys Chem* 1996, 100, 5813.

6. Tokuhashi, K.; Nagai, H.; Takahashi, A.; Kaise, M.; Kondo, S.; Sekiya, A.; Takahashi, M.; Gotoh, Y.; Suga, A. *J Phys Chem A* 1999, 103, 2664.
7. Chandra, A. K.; Uchimaru, T. *J Phys Chem A* 2000, 104, 8535.
8. Chandra, A. K.; Uchimaru, T. *J Phys Chem A* 1999, 103, 10874.
9. Albu, T. V.; Swaminathan, S. *J Phys Chem A* 2006, 110, 7663.
10. Albu, T. V.; Swaminathan, S. *Theor Chem Acc* 2007, 117, 383.
11. Espinosa-Garcia, J.; Coitino, E. L.; Gonzalez-Lafont, A.; Lluch, M. J. *J Phys Chem A* 1998, 102, 10715.
12. Fontana, G.; Causa, M.; Gianotti, V.; Marchionni, G. *J Fluorine Chem* 2001, 109, 113.
13. Gonzalez-Lafont, A.; Lluch, J. M.; Espinosa-Garcia, J. *J Phys Chem A* 2001, 105, 10553.
14. Korchowiec, J.; Kawahara, S.-I.; Matsumura, K.; Uchimaru, T.; Surgie, M. *J Phys Chem A* 1999, 103, 3548.
15. Schwartz, M.; Marshall, P.; Berry, R. J.; Ehlers, C. J.; Petersson, G. A. *J Phys Chem A* 1998, 102, 10074.
16. Zhang, M.; Lin, Z.; Song, C. *J Chem Phys* 2007, 126, 34307.
17. Espinosa-Garcia, J. *J Phys Chem A* 2002, 106, 5686.
18. Sekusak, S.; Sabljic, A. *J Phys Chem A* 1968, 2001, 105.
19. Wang, Y.; Liu, J.; Yang, L.; Zhao, X.; Ji, Y.; and Li, Z. *J Phys Chem A* 2007, 111, 7761.
20. Nelson, D. D.; Zahniser, M. S.; Kolb, C. E.; Magid, H. *J Phys Chem* 1995, 99, 16301.
21. Rajakumar, B.; Portman, R. W.; Burkholder, J. B.; Ravishankara, A. R. *J Phys Chem A* 2006, 110, 6724.
22. Percival, C. J.; Marston, G.; Wayne, R. P. *Atmos Environ* 1995, 29, 305.
23. Atkinson, R.; Baulch, D. L.; Cox, R. A.; Hampson, D. L., Jr.; Kerr, A. J.; Troe, J. *J Phys Chem Ref Data* 1992, 21, 1125.
24. De More, W. B.; Sander, S. P.; Golden, D. M.; Molina, M. J.; Hampson, R. F.; Kurylo, M. J.; Howard, C. J.; Ravishankara, A. R. *Chemical Kinetics and Photochemical Data for Use in Stratospheric Modeling*, JPL 90-1; Evaluation No. p, Pasadena, 1990.
25. Gonzalez-Lafont, A.; Lluch, J. M.; Varela-Alvarez, A.; Sordo, J. A. *J Phys Chem B* 2008, 112, 328.
26. Adamo, C.; Barone, V. *J Chem Phys* 1998, 108, 664.
27. Becke, A. D. *J Chem Phys* 1996, 104, 1040.
28. Zhao, Y.; Lynch, B. J.; Truhlar, D. G. *J Phys Chem A* 2004, 108, 2715.
29. Urata, S.; Takada, A.; Uchimaru, T.; Chandra, A. K. *Chem Phys Lett* 2003, 368, 215.
30. Moller, C.; Plesset, M. S. *Phys Rev* 1934, 46, 618.
31. Becke, A. D. *J Chem Phys* 1993, 82, 1372.
32. Lee, C.; Yang, W.; Parr, R. G. *Phys Rev B* 1988, 37, 785.
33. Stephens, P. J.; Devlin, F. J.; Chabalowski, C. F.; Frisch, M. J. *J Phys Chem* 1994, 98, 11623.
34. Hehre, W. J.; Paul, L. R.; Schleyer, V. R.; Pople, J. A. *Ab Initio Molecular Orbital Theory*; Wiley, New York, 1987.
35. Frisch, M. J.; Trucks, G. W.; Schlegel, H. B.; Scuseria, G. E.; Robb, M. A.; Cheeseman, J. R.; Montgomery, J. A., Jr.; Vreven, T.; Kudin, K. N.; Burant, J. C.; Millam, J. M.; Iyengar, S. S.; Tomasi, J.; Barone, V.; Mennucci, B.; Cossi, M.; Scalmani, G.; Rega, N.; Petersson, G. A.; Nakatsuji, H.; Hada, M.; Ehara, M.; Toyota, K.; Fukuda, R.; Hasegawa, J.; Ishida, M.; Nakajima, T.; Honda, Y.; Kitao, O.; Nakai, H.; Klene, M.; Li, X.; Knox, J. E.; Hratchian, H. P.; Cross, J. B.; Bakken, V.; Adamo, C.; Jaramillo, J.; Gomperts, R.; Stratmann, R. E.; Yazyev, O.; Austin, A. J.; Cammi, R.; Pomelli, C.; Ochterski, J. W.; Ayala, P. Y.; Morokuma, K.; Voth, G. A.; Salvador, P.; Dannenberg, J. J.; Zakrzewski, V. G.; Dapprich, S.; Daniels, A. D.; Strain, M. C.; Farkas, O.; Malick, D. K.; Rabuck, A. D.; Raghavachari, K.; Foresman, J. B.; Ortiz, J. V.; Cui, Q.; Baboul, A. G.; Clifford, S.; Cioslowski, J.; Stefanov, B. B.; Liu, G.; Liashenko, A.; Piskorz, P.; Komaromi, I.; Martin, R. L.; Fox, D. J.; Keith, T.; Al-Laham, M. A.; Peng, C. Y.; Nanayakkara, A.; Challacombe, M.; Gill, P. M. W.; Johnson, B.; Chen, W.; Wong, M. W.; Gonzalez, C.; and Pople, J. A. *Gaussian 03, Revision C. 02*; Gaussian, Inc.: Wallingford CT, 2004.
36. Dennington, I. I. R.; Keith, T.; Millam, J.; Eppinnett, K.; Hovell, W. L.; Gilliland, R. *GaussView, Version 3.09*; Semichem, Inc.: Shawnee Mission, KS, 2003.
37. Curtiss, L. A.; Redfern, P. C.; Raghavachari, K.; Rassolov, V.; Pople, J. A. *J Chem Phys* 1998, 109, 7764.
38. Curtiss, L. A.; Redfern, P. C.; Raghavachari, K.; Rassolov, V.; Pople, J. A. *J Chem Phys* 1999, 110, 4703.
39. Baboul, A. G.; Curtiss, L. A.; Redfern, P. C.; Raghavachari, K. *J Chem Phys* 1999, 110, 7650.
40. Wright, M. R. *Fundamental Chemical Kinetics and Exploratory Introduction to the Concepts*; Ellis Horwood: Chichester, 1999.
41. Ogura, T.; Miyoshi, A.; Koshi, M. *Phys Chem Chem Phys* 2007, 9, 5133.
42. Pollak, E.; Pechukas, P. *J Am Chem Soc* 1978, 100, 2984.
43. Gilbert, R. G.; Smith, S. C. *Theory of Unimolecular and Recombination Reactions*; Blackwell Scientific: Oxford, 1990.
44. Wigner, E. Z. *Phys Chem B* 1932, 19, 103.
45. Louis, F.; Gonzalez, C. A.; Huie, R. E.; Kurylo, M. J. *J Phys Chem A* 2000, 104, 8773.
46. Chuang, Y.; Truhlar, D. G. *J Chem Phys* 2000, 112, 1221.
47. Prinn, R.; Cunnold, D.; Simmonds, P.; Alyea, F.; Boldi, R.; Crawford, A.; Fraser, P.; Gutzler, D.; Hartley, D.; Rosen, R.; Rasmusseen, R. J. *J Geophys Res [Atmos]* 1992, 97, 2445.
48. Prinn, R.; Weiss, R.; Millar, B.; Jaung, J.; Alyea, F.; Cunnold, D.; Fraser, P.; Hartley, D.; Simmonds, P. *Science* 1995, 269, 187.